Heliyon 9 (2023) e16619

Contents lists available at ScienceDirect

Heliyon

journal homepage: www.cell.com/heliyon

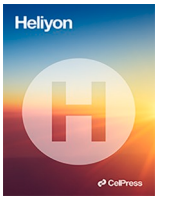

Research article

Gasdermin D affects aortic vascular smooth muscle cell pyroptosis and Ang II-induced vascular remodeling

Zimin Fang [b,1], Gaojun Wu [b,1], Jian Sheng [a,1], Bozhi Ye [b], Zhouqing Huang [b], Jianjiang Xu [a], Jianqin Zhang [a], Jibo Han [a], Bingjiang Han [a,**], Jiajun Xu [a,*]

[a] *Department of Cardiology and the Key Laboratory of Cardiovascular Disease of Jiaxing, The Second Affiliated Hospital of Jiaxing University, Jiaxing, Zhejiang, China*

[b] *Department of Cardiology and the Key Laboratory of Cardiovascular Disease of Wenzhou, The First Affiliated Hospital, Wenzhou Medical University, Wenzhou, Zhejiang, China*

A R T I C L E I N F O

Keywords:
Gasdermin D
Pyroptosis
Vascular smooth muscle cell
Vascular remodeling

A B S T R A C T

Vascular smooth muscle cells (VSMCs) are primarily responsible for vasoconstriction and the regulation of blood pressure1. Pyroptosis, a particular form of regulated cell death, is involved in multiple vascular injuries, including hypertensive vascular dysfunction. This pyroptotic cell death is mediated by the pore-forming protein of Gasdermin D (GSDMD). This study was designed to examine the direct effect of GSDMD on smooth muscle cell pyroptosis and vascular remodeling. Findings revealed that GSDMD was activated in Angiotensin (Ang) II- treated aortas. We then showed that genetic deletion of Gsdmd reduced vascular remodeling and aorta pyroptosis induced by Ang II *in vivo*. Aberrant expression of GSDMD by recombinant AAV9 virus carrying Gsdmd cDNA aggravated the level of pyroptosis in aortas of Ang II mice. Gain- and loss-of-function analysis further confirmed that GSDMD regulated the pyroptosis of murine aortic vascular smooth muscle cells (MOVAS) in an *in vitro* model of tumor necrosis factor (TNF)-α treatment, which was achieved by transfecting expressing plasmid or siRNA, respectively. Overall, this study provided evidence supporting the active involvement of GSDMD in smooth muscle cell pyroptosis and Ang II-induced mice vascular injury. This finding lends credence to GSDMD as a potential therapeutic target for hypertensive vascular remodeling via inhibiting pyroptosis.

1. Introduction

Vascular smooth muscle cells (VSMCs), a fundamental component of arterial media, are primarily responsible for vasoconstriction and the regulation of blood pressure [1]. It has become increasingly clear that VSMCs in a pathological state are involved in a variety of vascular injuries [2]. For instance, VSMCs undergo apoptosis and the degeneration of the aortic medial layer during aortic aneurysm [3]. VSMCs may also experience phenotypic switch, which has also been identified as a hallmark of vascular remodeling in atherosclerosis, hypertension, and diabetic vascular complications [4]. Moreover, a handful of studies have even documented the role of

* Corresponding author.
** Corresponding author.
E-mail addresses: binjianghanjx2y@163.com (B. Han), jiajunjx2y@163.com (J. Xu).
[1] Zimin Fang, Gaojun Wu and Jian Sheng contribute equally to this paper.

https://doi.org/10.1016/j.heliyon.2023.e16619
Received 26 November 2022; Received in revised form 18 May 2023; Accepted 23 May 2023
Available online 26 May 2023

VSMC pyroptosis in multiple vascular injuries, including atherosclerosis [5], aortic aneurysm [6], and vascular calcification [7].

Pyroptosis is a form of inflammatory programmed cell death that can be mediated by the inflammasome/Caspase1-dependent canonical pathway and the Caspase4(human)/11(mouse)- dependent non-canonical pathway [8,9]. First, inflammatory caspases shear Gasdermin D (GSDMD) to separate its N-domain (GSDMD-N) and C-domain. Then the GSDMD-N fragments are enriched to the plasma membrane, forming cytomembrane pores and releasing interleukin (IL)-1 and other inflammatory factors as well as cell content such as lactate dehydrogenase (LDH) [10,11]. GSDMD is widely expressed in different cell types and tissues, including all cell components of vessel walls, which supports the understanding that pyroptosis is not limited to inflammatory cells [12]. GSDMD works as the shared executor of two pathways for pyroptosis: canonical Caspase1 and non-canonical Caspase4/11, and is insensitive to apoptotic caspases [10,11]. Expression of the GSDMD-N is sufficient to induce pyroptosis in mammalian cells by forming membrane pores [10,11,13].

Initially, GSDMD-mediated pyroptosis was found to be associated with innate immune response, auto-immune disease and tumor drug resistance [14]. Recently, GSDMD activation and pyroptosis has been shown in multiple vascular injuries, including atherosclerosis [15], aortic aneurysm [16,17], and hypertensive vascular dysfunction [18]. However, the direct effect of GSDMD on smooth muscle cell pyroptosis and vascular remodeling remains unknown. Herein, our results provided evidence supporting the active involvement of GSDMD in smooth muscle cell pyroptosis and Ang II-induced mice vascular injury. They also lend credence to GSDMD as a potential therapeutic target that may be useful for hypertensive vascular remodeling via inhibiting VSMCs pyroptosis.

2. Methods and details

2.1. Animal experiments

Experimental protocols involving mice received ethical approval from the Second Affiliated Hospital of Jiaxing University ethics committee (approval document no. 2021JX044) and strictly followed National Institutes of Health guidelines (Guide for the care and use of laboratory animal, USA). Male *Gsdmd*-knockout mice (*Gsdmd*$^{-/-}$, Strain NO.T010437) with a C57BL/6J background and littermate wild-type mice were obtained from Gempharmatech (Nanjing, China). *Gsdmd*$^{-/-}$ mice were generated by CRISPR/Cas9 system as described in our previous publication [19]. Two guide RNAs (sgRNA, designing by an online CRISPR design tool: http://crispr.mit.edu)- targeting introns were constructed on both sides of the *Gsdmd* region separately. Then Cas9 mRNA was injected into zygotes simultaneously with sgRNA. Knockout efficiency of *Gsdmd* was also verified in our previous publication [19]. 6–8 weeks old male wildtype mice and *Gsdmd*$^{-/-}$ mice were assigned into 5 groups through randomization: wildtype group (WT, n = 6), *Gsdmd*$^{-/-}$ group (*Gsdmd*$^{-/-}$, n = 6), wildtype + Ang II group (WT + Ang II, n = 6), *Gsdmd*$^{-/-}$ + Ang II group (*Gsdmd*$^{-/-}$ + Ang II, n = 6), and over-expression of GSDMD + Ang II group (*Gsdmd*^{OE} + Ang II, n = 6). For studies involving *Gsdmd*^{OE}, mice were injected with recombinant AAV9 virus carrying *Gsdmd* cDNA (AAV9-*CMV-Gsdmd-3flag*-EGFP) through tail vein at a total dose of 3E+11 vg. Other groups received an equal volume of vehicle (AAV9-*CMV-Empty*). After 4 weeks, Ang II or PBS osmotic mini-pumps were administered. For vascular remodeling, osmotic mini-pumps (Alzet MODEL 1004, Durect Corporation, CA) loaded with Ang II (1000 ng/kg/min, HY-13948, MedChemExpress) were subcutaneously implanted into the mice, which lasted for 4 weeks.

A tail-cuff pressure analysis system (BP-2010A; Softron, Japan) was used to assess systolic blood pressure (SBP) at the indicated time non-invasively. After the treatment, the mice were euthanized under sodium pentobarbital anesthesia, and their aortic tissues were preserved.

2.2. Immunostaining

Immunofluorescent double-staining of optical cutting temperature compound (OCT) sections was performed by incubating them with both anti-GSDMD (sc-393581, Santa Cruz, 1:200) and anti-αSMA (ab7817, Abcam, 1:200) or anti-CD31 (a marker of vascular endothelial cells, ab281583, Abcam, 1:200), followed by incubation with TRITC-labeled (ab6786, Abcam, 1:500) or Alexa Fluor488-labeled (ab150077, Abcam, 1:500) secondary antibodies. A fluorescence microscope (Leica, Germany) was employed to capture the images. The observer was blinded to the results.

For immunohistochemical staining, OCT-embedded tissues were first fixed in cold pure methanol. After the fixing, they were permeabilized with 0.25% Triton-X for 10 min, and finally blocked with 5% bovine serum albumin (BSA) for 30 min. Anti-COL-3 (sc-518017, Santa Cruz, 1:200) incubation was conducted at 4 °C overnight, following which was 1 h room-temperature incubation with secondary antibody (1:200). Immunoreactivity was detected by diaminobenzidine (DAB). Hematoxylin was used to counterstain sections. Brightfield microscopy (Nikon, Japan) was used to image the stained sections. The observer was blinded to the results.

2.3. Histological assessments

To prepare for intima-media thickness analysis, 5 μm OCT-embedded aortic tissue sections underwent hematoxylin and eosin (HE) staining. In order to assess fibrosis, the OCT-embedded sections were subjected to staining with Masson's trichome. According to the manufacturer's operating procedures, TUNEL staining (C1091, Beyotime Biotechnology, China) was also applied to aortic sections to evaluate cell death with nucleus DNA damage. The stained sections were examined under brightfield microscopy (Nikon, Japan). Randomly visual fields were captured by an observer blind to the allocation of treatment.

2.4. Cell culture, transfection and viability

We obtained MOVAS and HUVECs from the Shanghai Institute of Biochemistry and Cell Biology (Shanghai, China) and cultured them in DMEM (C11995500BT, Gibco, Germany) containing fetal bovine serum (10%, 10099141C, Gibco, Germany), 100 U/ml streptomycin-penicillin (P1400, Solarbio, China). Before experimental operation, cultured cells were serum-starved.

Our transfection strategy is based on the comprehensive consideration of transfection efficiency, cell toxicity, easy-to-operate and economy in accordance with our previous practical cases [19,20]. GSDMD was silenced in MOVAS through small interfering RNA (siRNA, 5'-GCCTCCATGAATGTGTGTA-3', Ribobio, China) under LipofectAMINE™ 2000 (Invitrogen). Over-expression of GSDMD-N in MOVAS was achieved by encoding plasmid (Genechem) under LipofectAMINE™ 3000 (Invitrogen). Transfection efficiency was determined by immunoblotting. For transfection, seeding cells to be 70–90% confluent at transfection, diluting LipofectAMINE reagent in Opti-medium (2 μl for 6-well) for 5 min, diluting siRNA (3 μl for 6-well) or plasmid (1 μg for 6-well) in Opti-medium for 5 min, adding diluted siRNA or plasmid to diluted LipofectAMINE reagent (1:1 ratio) for 15 min, adding siRNA or plasmid-lipid complex to cells, and incubating cells for 1 day at 37 °C.

CCK 8 assay was conducted in accordance with the manufacturer's operating protocols to assess cell viability (Dojindo Laboratories, Japan).

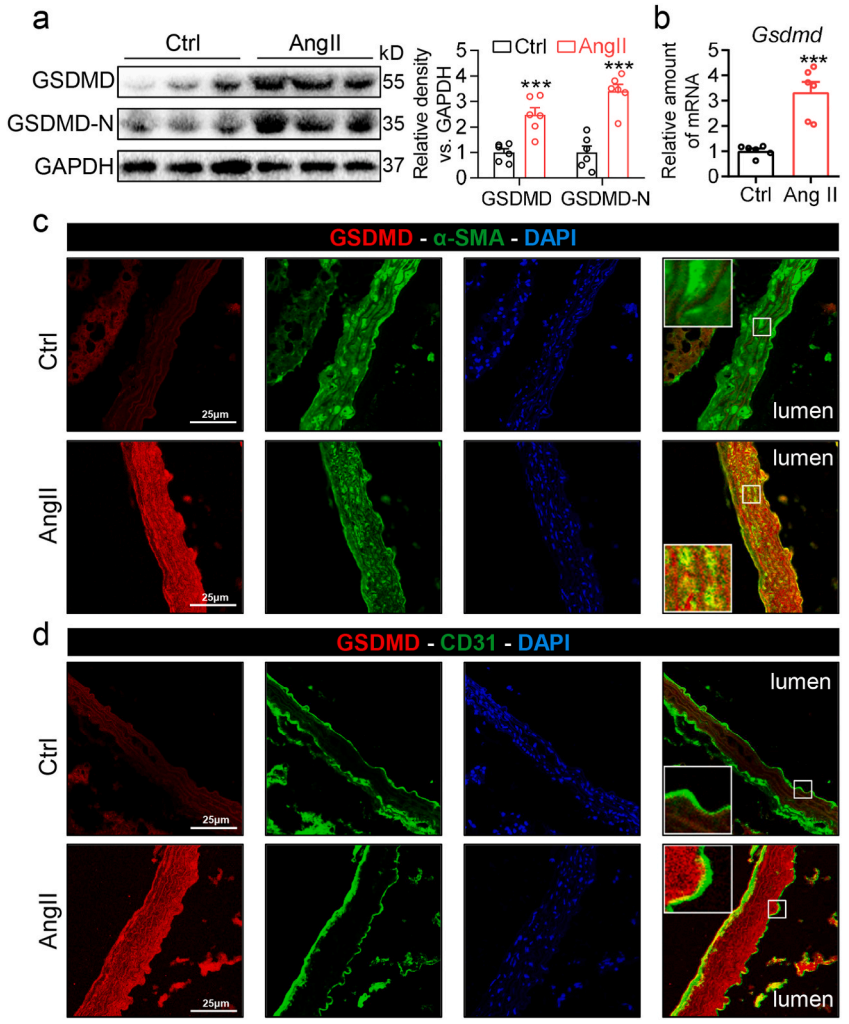

Fig. 1. GSDMD is increased in aortic tissues of Ang II-induced mice. (**a**) Protein levels of GSDMD (full length) and GSDMD-N (N-terminal) were detected in aortic tissues from Ang II-induced hypertensive mice. Densitometric quantification of the immunoblot. Full, non-adjusted images of bots were shown in supplementary material. (**b**) mRNA level of *Gsdmd* was detected in aortic tissue lysates. (**c-d**) Representative double-immunofluorescence staining images of aortic tissues from Ang II-infused mice, showing immunoreactivity to GSDMD (red), smooth muscle cell marker α-SMA (green, **c**), or endothelial cell marker CD31 (green, **d**). Merged images (yellow) showing colocalization (n = 6 for each group; *, vs. Ctrl group; ***P < 0.001). (For interpretation of the references to colour in this figure legend, the reader is referred to the Web version of this article.)

2.5. Fluorescent staining of propidium iodide (PI)

Pyroptosis was determined by Hoechst and PI double fluorescent staining. MOVAS first underwent 10 min Hoechst (3 μg/mL) staining, followed by a 15 min staining with PI (1 μg/mL). Hoechst staining was also applied to the cell nuclei, and pyroptosis cells were labeled with PI by entry through ruptured cell membranes. The images were captured with a fluorescence microscope (Leica,

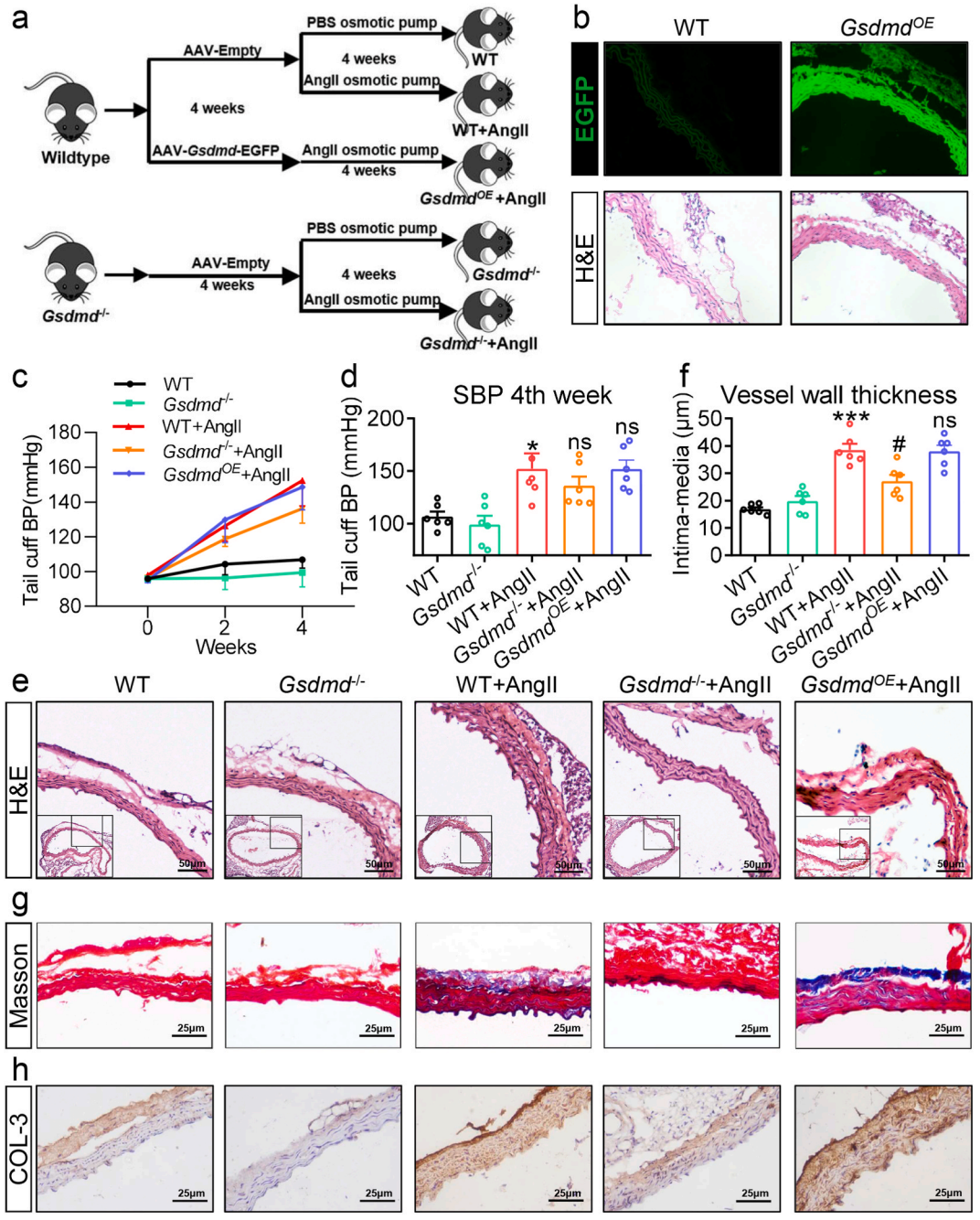

Fig. 2. Gsdmd$^{-/-}$ protects against Ang II-induced vascular remodeling. (**a**) The animal experiments flowchart. (**b**) Representative images of GSDMD immunofluorescence staining (EGFP, **upper**) and H&E staining (**below**) of aortic tissues. Mice systolic blood pressure (SBP) during study (**c**) and at termination of study (**d**). (**e**) Representative images of H&E staining of aortic tissues from wild-type, *Gsdmd*$^{-/-}$, and *Gsdmd*^{OE} mice with or without Ang II infusion. (**f**) Quantification of vessel wall thickness. (**g**) Representative images of Masson's trichome staining. (**h**) Representative images of immunohistochemical staining for COL-3 (n = 6 for each group; *, vs. Ctrl group; # and ns, vs. Ang II group; * and #P < 0.05, ***P < 0.001; ns = no significance).

Germany). Randomly visual fields were captured by an observer blind to the allocation of treatment.

2.6. Measurement of cytokines and LDH

Mouse aortic tissues or cell supernatants were collected and determined by IL-1β ELISA kit (eBioscence, San Diego, CA) in strict compliance with the manufacturer's operating protocols. LDH assay kits were employed to measure the release of LDH into the culture media (C0016, Beyotime Biotechnology, China) and LDH activity in aortic tissues (BC0685, Solarbio Biotechnology, China) in strict compliance with the manufacturer's instructions.

2.7. Western blot analysis

The routine Western blot procedures were implemented similarly as previously described [21,22]. Primary antibody against GSDMD (ab219800, 1:1000) was obtained from Abcam. Anti-Flag (20543-1-AP, 1:1000) was procured from Proteintech. Antibody against GAPDH (5174, 1:1000) and the secondary horseradish peroxidase-conjugated antibody were obtained from CST. Images were analyzed using Image Lab 5.2 by an observer blind to the allocation of treatment.

2.8. Statistical analysis

All *in vitro* or *in vivo* results were expressed in the form of means ± standard error of the mean (SEM) in this study. To identify group differences, unpaired student's t-test was applied (2 group studies). For >2 groups, we used one way-ANOVA with multiple comparisons (Bonferroni's correction). $P < 0.05$ was used as the criterion for determining statistical significance. All analyses were executed with GraphPad Pro Prism 8.0 (GraphPad, San Diego, CA).

3. Results

3.1. GSDMD expression is elevated in hypertensive aortas

To clarify how GSDMD affects hypertensive aortic injury, we subcutaneously implanted Ang II osmotic mini-pumps (1.44 mg/kg/day) in mice to induce hypertensive vascular remodeling as our previous research [23]. Western blot analysis showed an increase in GSDMD expression and cleavage in the aortas of Ang II mice (Fig. 1a). The mRNA level of *Gsdmd* was also significantly increased after modeling (Fig. 1b). To further study the cellular origin of GSDMD in hypertensive aortas, the aortic tissue sections were taken for double-immunofluorescence staining. The immunofluorescence results consistently pointed to upregulated GSDMD expression in Ang II-induced vascular remodeling (Fig. 1c–d). In addition, GSDMD was mainly expressed in the α-SMA-positive smooth muscle cells (Fig. 1c), rather than in CD31-positive vascular endothelium (Fig. 1d). The above results suggest that GSDMD might be a potential regulator of hypertensive aortic injury.

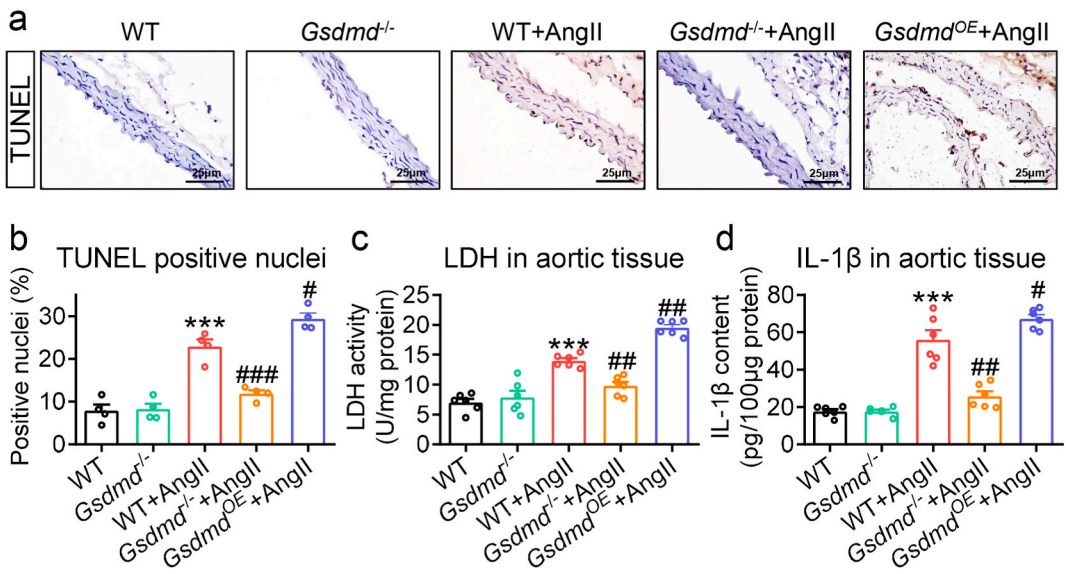

Fig. 3. Involvement of GSDMD in Ang II-induced aorta pyroptosis *in vivo*. (**a**) Representative images of TUNEL staining of aortic tissues from wild-type and *Gsdmd*$^{-/-}$ mice with or without Ang II infusion. (**b**) Quantification of TUNEL staining in Fig. 3a is shown. (**c**) The level of LDH in aortic tissues was detected by assay kit. (**d**) Protein level of IL-1β in aortic tissues of Ang II model was determined by ELISA kit (n = 6 for each group; *, vs. Ctrl group; #, vs. Ang II group; #P < 0.05, ##P < 0.01, *** and ###P < 0.001).

3.2. Loss of GSDMD aggravates Ang II-induced vascular remodeling in vivo

To investigate the function of GSDMD in hypertensive aortic injury, we used GSDMD knockout (*Gsdmd*$^{-/-}$) and GSDMD over-expressed (*Gsdmd*^{OE}) mice. *Gsdmd*^{OE} mice were developed by recombinant AAV9 virus carrying *Gsdmd* cDNA (AAV9-*CMV-Gsdmd-3flag*-EGFP). Then, mice were implanted with Ang II or PBS osmotic mini-pumps subcutaneously (flowchart in Fig. 2a). Immunofluorescence staining showed that the protein content of GSDMD in vessels injected with AAV9-*CMV-Gsdmd-3flag*-EGFP was increased compared to that in AAV9-*CMV-Empty* control mice (WT) (Fig. 2b). The hypertensive model mice showed increased systolic blood pressure (SBP) (Fig. 2c–d), whereas a null difference in blood pressure was recorded among hypertensive WT, *Gsdmd*$^{-/-}$, and *Gsdmd*^{OE} mice (Fig. 2c–d, $p > 0.05$). H&E analysis of aortic wall thickness (Fig. 2e–f), Masson's trichome staining for fibrosis (Fig. 2g) and COL-3 staining for collagen deposition (Fig. 2h) showed aggravated remodeling in mice subcutaneously implanted with Ang II pumps. *Gsdmd*$^{-/-}$ protected against vascular remodeling in Ang II-operated mice (Fig. 2e–h), whereas *Gsdmd*^{OE} did not affect such Ang II effect (protect or aggravate). The above results indicated that *Gsdmd*$^{-/-}$ mice exhibited less vascular damage and GSDMD might be a therapeutic target for hypertensive aortic injury.

3.3. Involvement of GSDMD in aortic pyroptosis of Ang II-infused mice

Since *Gsdmd*$^{-/-}$ showed a protective effect on Ang II-induced aortic injury, the next step was to assess whether deficiency (*Gsdmd*$^{-/-}$) or aberrant expression (*Gsdmd*^{OE}) would yield a functional change in pyroptosis as well. Fig. 3 a-b showed that Ang II led to increased TUNEL-positive nuclei in aortic tissues, an occurrence that is typical characteristic of pyroptosis. In *Gsdmd*$^{-/-}$ mice, this change was abolished, contrary to its increase in *Gsdmd*^{OE} mice (Fig. 3 a-b). Similarly, we found that *Gsdmd*$^{-/-}$ significantly reduced and *Gsdmd*^{OE} significantly aggravated the LDH level in aortas of Ang II mice (Fig. 3 c). These results are congruent with aortic IL-1β content, which were significantly dampened in *Gsdmd*$^{-/-}$ + Ang II and elevated in *Gsdmd*^{OE} + Ang II mice (Fig. 3 d). The above results verified the involvement of GSDMD in vascular pyroptosis of Ang II mice from both sides.

3.4. GSDMD-mediated pyroptosis was elevated in TNF-α induced murine aortic vascular smooth muscle cells (MOVAS)

Based on the results that GSDMD expression is mainly distributed in VSMCs (Fig. 1c–d), we used cultured murine aortic vascular smooth muscle cells (MOVAS) to simulate the *in vitro* model. To detect pyroptosis in smooth muscle cells, MOVAS were exposed to 1 μM Ang II (consistent with the *in vivo* model) or 100 ng/mL TNF-α (induce vascular pyroptosis [6,24]) for 3, 6, 9, 12, 24, or 36 h, and

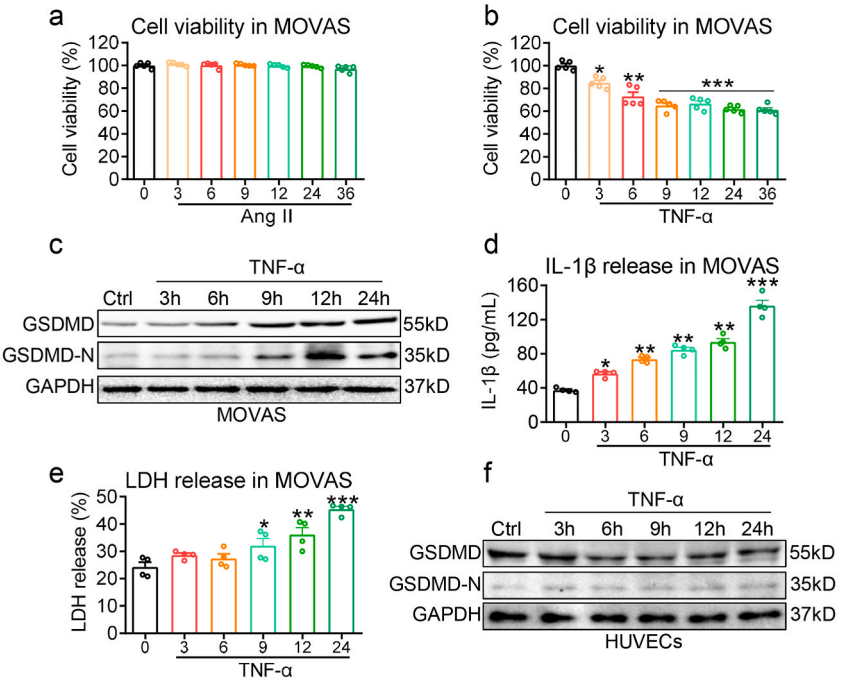

Fig. 4. GSDMD-mediated pyroptosis was elevated in TNF-α induced MOVAS. (**a-b**) MOVAS was treated with Ang II (1 μM) or TNF-α (100 ng/mL) for indicated time and were then measured for cell viability by CCK8 assay. (**c**) The protein expression of GSDMD (full length) and GSDMD-N (N-terminal) in MOVAS was detected by immunoblot. Full, non-adjusted images of bots were shown in supplementary material. (**d-e**) Release of IL-1β and LDH in MOVAS was detected. (**f**) HUVECs were treated with TNF-α (100 ng/mL) for indicated time and were then detected for the expression of GSDMD and GSDMD-N. Full, non-adjusted images of bots were shown in supplementary material (n = 5 for a, b, n = 4 for d, e; *, vs. Ctrl group; *P < 0.05, **P < 0.01, ***P < 0.001).

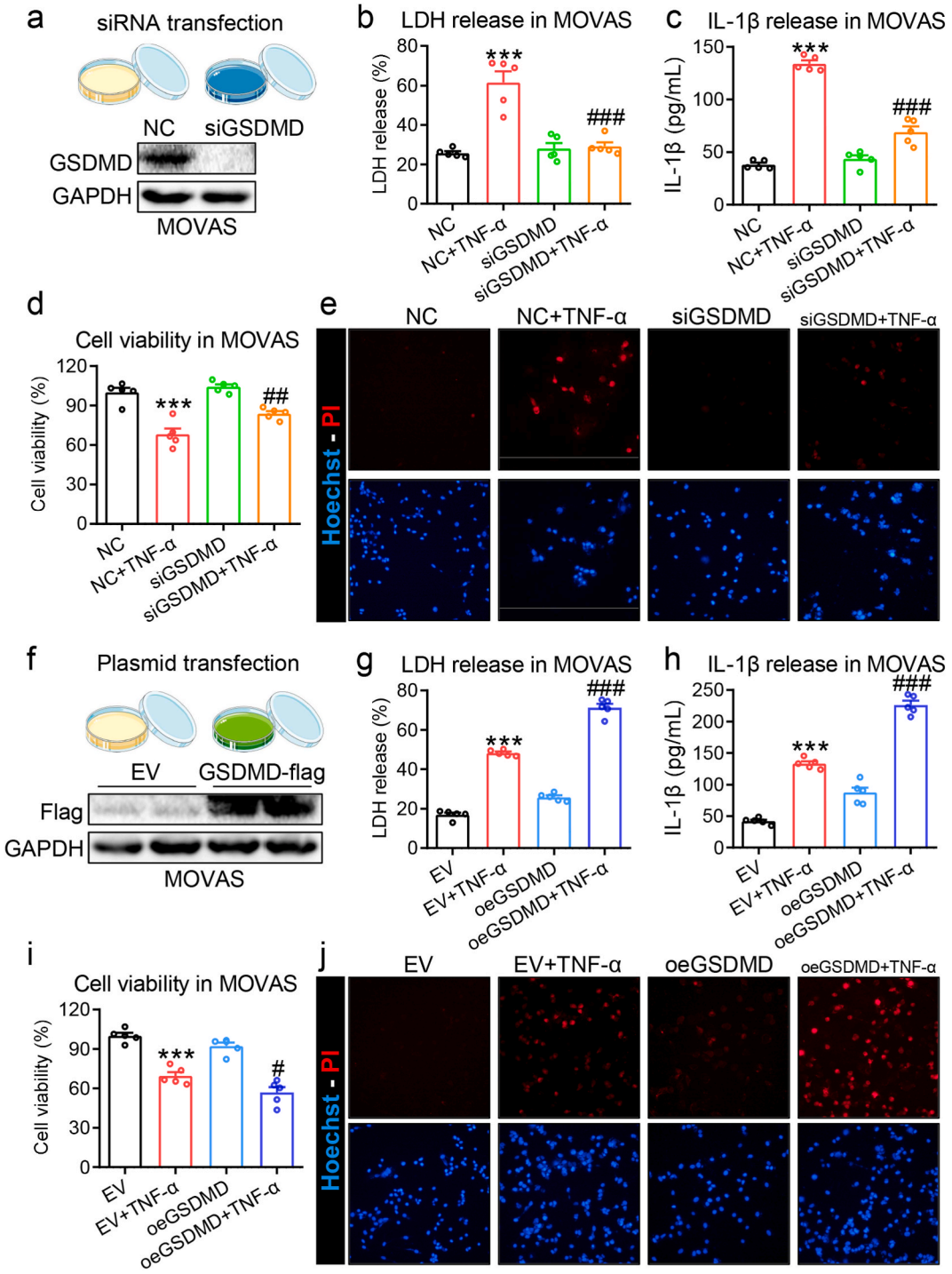

Fig. 5. Effect of silencing or overexpressing GSDMD on TNF-α induced MOVAS pyroptosis. (**a**) Immunoblot of GSDMD following siRNA GSDMD (siGSDMD) or negative control (NC) transfection in MOVAS. Full, non-adjusted images of bots were shown in supplementary material. NC and siGSDMD MOVAS were stimulated with TNF-α (100 ng/mL) for 24 h. (**b-c**) Release of IL-1β and LDH in MOVAS was detected. (**d**) Cell viability was measured in MOVAS by CCK8 assay. (**e**) One typical characteristic of pyroptosis was detected in MOVAS by PI (red) and Hoechst (blue) staining. (**f**) Immunoblot of Flag following GSDMD-flag expressing plasmid transfection (oeGSDMD) in MOVAS (EV = empty vehicle). Full, non-adjusted images of bots were shown in supplementary material. EV and oeGSDMD MOVAS were stimulated with TNF-α (100 ng/mL) for 24 h. Cell viability (**i**), release of IL-1β (**g**) and LDH (**h**) in MOVAS were detected. (**j**) Representative images of PI (red) and Hoechst (blue) double fluorescent staining (n = 5 for each group; *, vs. NC or EV group; #, vs. NC + TNF-α or EV + TNF-α group; #P < 0.05, ##P < 0.01, *** and ###P < 0.001). (For interpretation of the references to colour in this figure legend, the reader is referred to the Web version of this article.)

cell viability was measured. We found a null effect of Ang II on the cell viability of MOVAS (Fig. 4a), while TNF-α significantly reduced cell viability (Fig. 4b). Therefore, we selected TNF-α as the stimulator for *in vitro* experiments. According to Fig. 4c, TNF-α increased the protein expression and cleavage of GSDMD during 9–24 h. In addition, we found that 100 ng/mL TNF-α led to the release of significantly more pro-inflammatory cytokine IL-1β (Fig. 4d). Moreover, we further found that TNF-α markedly promoted the release of LDH to cellular supernatant (Fig. 4e). However, we found that TNF-α did not alter the expression and cleavage of GSDMD in HUVECs by Western blot (Fig. 4f). In a nutshell, TNF-α induced GSDMD activation and pyroptosis in aortic vascular smooth muscle cells.

3.5. Gain- and loss-of-function analysis of GSDMD in TNF-α induced MOVAS pyroptosis

To assess the loss-of-function of GSDMD in TNF-α-induced pyroptosis of smooth muscle cells, MOVAS were transfected with negative control (NC) or GSDMD siRNA (siGSDMD), and then the transfection efficiency was determined by Western blot (Fig. 5a). siGSDMD significantly suppressed the cellular supernatant LDH activity in TNF-α-induced MOVAS (Fig. 5b). In addition, GSDMD silencing led to less IL-1β being released in TNF-α-induced MOVAS (Fig. 5c). Further experiments found that siGSDMD markedly increased cell viability (Fig. 5d) and decreased the quantity of PI-positive nuclei (Fig. 5e) in TNF-α-induced MOVAS. Analogous to the loss-of-function assessment of GSDMD, the gain-of-function of GSDMD was evaluated by transfecting MOVAS with GSDMD-flag expressing plasmid (oeGSDMD) or empty vehicle plasmid (EV). Transfection efficiency was also measured by means of Western blot (Fig. 5f). Our results showed that oeGSDMD resulted in the release of more IL-1β (Fig. 5g) and LDH (Fig. 5h) in TNF-α-induced MOVAS. We further found that GSDMD overexpression decreased the cell viability (Fig. 5i) and elevated the quantity of PI-positive nuclei (Fig. 5j) in TNF-α-induced MOVAS. Gain- and loss-of-function analysis revealed that GSDMD mediated TNF-α-induced MOVAS pyroptosis.

4. Discussion

In this study, GSDMD was activated in Ang II-operated aortas. *Gsdmd*$^{-/-}$ inhibited hypertension-induced vascular remodeling and aorta pyroptosis *in vivo*. GSDMD overexpression aggravated the level of pyroptosis in aortas of Ang II mice. Gain- and loss-of- function analysis further confirmed that GSDMD regulated VSMCs pyroptosis in an *in vitro* model of TNF-α treatment. A summary of the major findings is presented in Fig. 6.

As a particular form of regulated cell death, pyroptosis is often manifested by the swelling of cells and release of inflammatory factors [8,9]. This pyroptotic cell death is mediated by the pore-forming GSDMD protein, which is cleaved by Caspase-1 or Caspase-4 (human)/11(mouse), followed by water influx, the release of cell content and ultimately cell lysis [10,11]. It is increasingly recognized that unregulated cell death through membrane pore formation contributes to chronic inflammatory diseases, which could be a cause or a consequence during chronic diseases [14]. As a fundamental component of arterial media, VSMCs pyroptosis has been increasingly implicated in the pathogenesis of aortic aneurysm [6,25], vascular calcification [7], and atherosclerosis [5]. Pyroptosis effector GSDMD was activated in mouse aortic smooth muscle cells treated with TNF-α and abdominal aorta of Ang II-induced abdominal aortic aneurysm (AAA) models [6]. Moreover, the activation of α7 nicotinic acetylcholine receptor (α7nAChR) showed a positive effect by protecting the AAA of Ang II-induced ApoE$^{-/-}$ mice via blockade of NLRP3/caspase-1/GSDMD pathway [6]. A single cell RNA-sequencing analysis of aortic degeneration and dissection (ADD) showed that aortic challenge resulted in upregulated expression of pyroptosis-associated key genes in a cluster of VSMCs, such as *Zbp1*, *Gsdmd*, *Casp1*, and *Casp4* [25]. Moreover, in a β-glycerophosphate induced calcification model, the expression of pyroptosis-associated proteins and pyroptotic cell death were increased in VSMCs [7]. The above studies suggest a possible link between VSMCs pyroptosis and vascular injuries.

Various stress and pathological conditions can promote vascular remodeling, including hypertension [26], atherosclerosis [27], and obesity [28,29]. In our previous study, we found evidence that high-fat diet could activate TLR4/MD2-regulated vascular

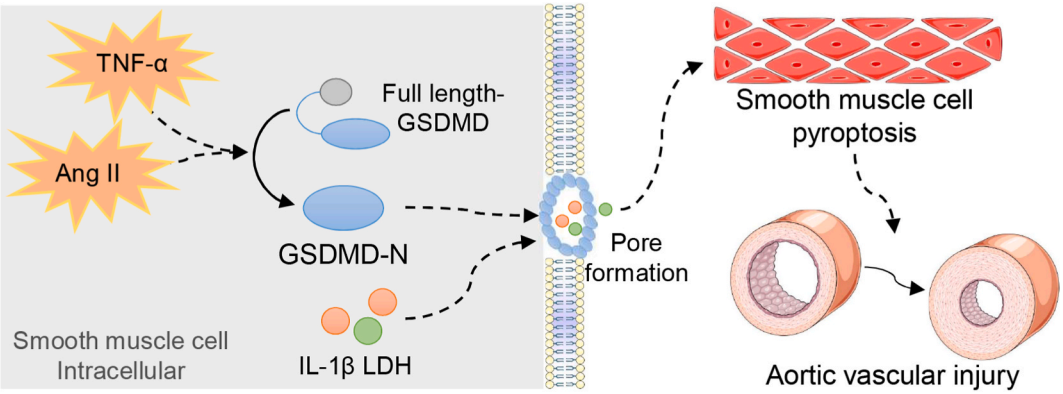

Fig. 6. Schematic illustration of the role of GSDMD on smooth muscle cell pyroptosis. During Ang II-induced aortic vascular remodeling or TNF-α-induced *in vitro* model, GSDMD was activated and mediated pyroptosis in aortas or MOVAS via perforating plasma membrane and promoting the release of IL-1β and LDH.

oxidative stress and promote fibrosis, and remodeling *in vivo* [29]. Ang II is the primary element of the renin-angiotensin system that is closely connected with hypertensive vascular remodeling. VSMC dysfunction (such as phenotypic transformation and apoptosis) [4], inflammation, and endothelial to mesenchymal transition (EndMT) [30] have been partly accepted as pathophysiological processes of vascular remodeling in hypertension. However, it is not known whether GSDMD and associated pyroptosis are involved in Ang II-induced vascular remodeling. The results of our study complement these findings by demonstrating that GSDMD expression is elevated in hypertensive aortas. Accordingly, we found that genetic deletion of *Gsdmd* decreased Ang II-induced vascular remodeling and aorta pyroptosis *in vivo*. Under saturating conditions with GSDMD overexpression, Ang II mice showed aggravated level of pyroptosis.

We firstly selected Ang II as the stimulus *in vitro* experiment, which is more consistent with the pathophysiological mechanism of vascular remodeling and our *in vivo* model. In contrast, Ang II had no effect on cell viability of MOVAS, contrary to its decrease under TNF-α treatment. TNF-α has been proved to cause pyroptosis in smooth muscle cells *in vitro* [6]. In line with this observation, TNF-α also increased the level of pyroptosis, as evidenced by the activation of GSDMD, release of IL-1β, and pyroptotic cell death (LDH release and PI-positive nuclei increase). To assess the gain- and loss-of-function of GSDMD in TNF-α-induced smooth muscle cell pyroptosis, transfection was performed in MOVAS with GSDMD siRNA or GSDMD-flag expressing plasmid, which proved that GSDMD mediated TNF-α-induced MOVAS pyroptosis.

In summary, our findings indicate that GSDMD has a direct impact on TNF-α-induced smooth muscle cell pyroptosis and Ang II-induced vascular remodeling. This serves as promising evidence that GSDMD may have the potential to be used as a therapeutic target for hypertensive vascular remodeling via inhibiting VSMCs pyroptosis.

Author contribution statement

Zimin Fang: Performed the experiments; Analyzed and interpreted the data.
Gaojun Wu: Performed the experiments; Analyzed and interpreted the data; Contributed reagents, materials, analysis tools or data.
Jian Sheng: Bozhi Ye: Performed the experiments; Contributed reagents, materials, analysis tools or data.
Zhouqing Huang: Performed the experiments.
Jianjiang Xu: Jianqin Zhang: Conceived and designed the experiments.
Jibo Han: Analyzed and interpreted the data; Contributed reagents, materials, analysis tools or data.
Bingjiang Han: Conceived and designed the experiments; Analyzed and interpreted the data; Contributed reagents, materials, analysis tools or data; Wrote the paper.
Jiajun Xu: Conceived and designed the experiments; Contributed reagents, materials, analysis tools or data; Wrote the paper.

Data availability statement

Data included in article/supp. material/referenced in article.

Funding

This study was supported by the grants from the Science and Technology Bureau of Jiaxing city, Zhejiang, China (No.2021AY30012 to B.J. Han, No.2019AD32229 to J. Sheng), the Natural Science Foundation of Zhejiang Province (No. LGD21H020003 to J.B. Han, No. LQ21H020009 to B.Z. Ye), and the National Natural Science Foundation of China (No. 82271347 to G.J. Wu, No. 82003750 to B.Z. Ye).

Declaration of competing interest

The authors declare that they have no known competing financial interests or personal relationships that could have appeared to influence the work reported in this paper.

Appendix A. Supplementary data

Supplementary data to this article can be found online at https://doi.org/10.1016/j.heliyon.2023.e16619.

References

[1] P. Lacolley, V. Regnault, P. Segers, S. Laurent, Vascular smooth muscle cells and arterial stiffening: relevance in development, aging, and disease, Physiol. Rev. 97 (4) (2017) 1555–1617.
[2] J. Shi, Y. Yang, A. Cheng, G. Xu, F. He, Metabolism of vascular smooth muscle cells in vascular diseases, Am. J. Physiol. Heart Circ. Physiol. 319 (3) (2020) H613–h631.
[3] R.A. Quintana, W.R. Taylor, Cellular mechanisms of aortic aneurysm formation, Circ. Res. 124 (4) (2019) 607–618.
[4] B.N. Davis-Dusenbery, C. Wu, A. Hata, Micromanaging vascular smooth muscle cell differentiation and phenotypic modulation, Arterioscler. Thromb. Vasc. Biol. 31 (11) (2011) 2370–2377.

[5] P. Puylaert, M. Van Praet, Gasdermin D deficiency limits the transition of atherosclerotic plaques to an inflammatory phenotype in ApoE knock-out mice, Biomedicines 10 (5) (2022).
[6] H. Fu, Q.R. Shen, Y. Zhao, M. Ni, C.C. Zhou, J.K. Chen, et al., Activating α7nAChR ameliorates abdominal aortic aneurysm through inhibiting pyroptosis mediated by NLRP3 inflammasome, Acta Pharmacol. Sin. 25 (2022).
[7] Q. Pang, P. Wang, Irisin protects against vascular calcification by activating autophagy and inhibiting NLRP3-mediated vascular smooth muscle cell pyroptosis in chronic kidney disease, Cell Death Dis. 13 (3) (2022) 283.
[8] K. Nobuhiko, W. Søren, L. Mohamed, V.W. Lieselotte, L. Salina, D. Jennifer, et al., Non-canonical inflammasome activation targets caspase-11, Nature 479 (7371) (2011) 117.
[9] E.A. Miao, I.A. Leaf, P.M. Treuting, D.P. Mao, M. Dors, A. Sarkar, et al., Caspase-1-induced pyroptosis is an innate immune effector mechanism against intracellular bacteria, Nat. Immunol. 11 (12) (2010) 1136–1142.
[10] K. Nobuhiko, I.B. Stowe, B.L. Lee, O.R. Karen, A. Keith, Søren W, et al., Caspase-11 cleaves gasdermin D for non-canonical inflammasome signalling, Nature 526 (7575) (2015) 666–671.
[11] J. Shi, Y. Zhao, K. Wang, X. Shi, Y. Wang, H. Huang, et al., Cleavage of GSDMD by inflammatory caspases determines pyroptotic cell death, Nature 526 (7575) (2015) 660–665.
[12] N. Saeki, Y. Kuwahara, H. Sasaki, H. Satoh, T. Shiroishi, Gasdermin (Gsdm) localizing to mouse Chromosome 11 is predominantly expressed in upper gastrointestinal tract but significantly suppressed in human gastric cancer cells, Mamm. Genome : Off. J. Int. Mammal. Gen. Soci. 11 (9) (2000) 718–724.
[13] J. Ding, K. Wang, W. Liu, Y. She, Q. Sun, J. Shi, et al., Pore-forming activity and structural autoinhibition of the gasdermin family, Nature 535 (7610) (2016) 111.
[14] P. Yu, X. Zhang, N. Liu, L. Tang, C. Peng, X. Chen, Pyroptosis: mechanisms and diseases, Signal Transduct. Targeted Ther. 6 (1) (2021) 128.
[15] Z. Qian, Y. Zhao, C. Wan, Y. Deng, Y. Zhuang, Y. Xu, et al., Pyroptosis in the initiation and progression of atherosclerosis, Front. Pharmacol. 12 (2021), 652963.
[16] A. Chakraborty, Y. Li, C. Zhang, Y. Li, S.A. LeMaire, Y.H. Shen, Programmed cell death in aortic aneurysm and dissection: a potential therapeutic target, J. Mol. Cell. Cardiol. 163 (2022) 67–80.
[17] Y. Chen, Y. He, X. Wei, D.S. Jiang, Targeting regulated cell death in aortic aneurysm and dissection therapy, Pharmacol. Res. 176 (2022), 106048.
[18] C. De Miguel, P. Pelegrín, Emerging role of the inflammasome and pyroptosis in hypertension, Int. J. Mol. Sci. 22 (3) (2021).
[19] B. Ye, X. Shi, J. Xu, S. Dai, J. Xu, X. Fan, et al., Gasdermin D mediates doxorubicin-induced cardiomyocyte pyroptosis and cardiotoxicity via directly binding to doxorubicin and changes in mitochondrial damage, Transl. Res. 248 (2022) 36–50.
[20] J. Han, S. Dai, L. Zhong, X. Shi, X. Fan, X. Zhong, et al., GSDMD (gasdermin D) mediates pathological cardiac hypertrophy and generates a feed-forward amplification cascade via mitochondria-STING (stimulator of interferon genes) Axis, Hypertension 79 (11) (2022) 2505–2518.
[21] J. Han, S. Ye, C. Zou, T. Chen, J. Wang, J. Li, et al., Angiotensin II causes biphasic STAT3 activation through TLR4 to initiate cardiac remodeling, Hypertension 72 (6) (2018) 1301–1311.
[22] J. Han, C. Zou, L. Mei, Y. Zhang, Y. Qian, S. You, et al., MD2 mediates angiotensin II-induced cardiac inflammation and remodeling via directly binding to Ang II and activating TLR4/NF-kappaB signaling pathway, Basic Res. Cardiol. 112 (1) (2017) 9.
[23] J. Han, X. Shi, Y. Du, F. Shi, B. Zhang, Z. Zheng, et al., Schisandrin C targets Keap1 and attenuates oxidative stress by activating Nrf2 pathway in Ang II-challenged vascular endothelium, Phytother Res. 33 (3) (2019) 779–790.
[24] F. Yao, Z. Jin, Z. Zheng, X. Lv, L. Ren, J. Yang, et al., HDAC11 promotes both NLRP3/caspase-1/GSDMD and caspase-3/GSDME pathways causing pyroptosis via ERG in vascular endothelial cells, Cell Death Discovery 8 (1) (2022) 112.
[25] W. Luo, Y. Wang, L. Zhang, P. Ren, C. Zhang, Y. Li, et al., Critical role of cytosolic DNA and its sensing adaptor STING in aortic degeneration, dissection, and rupture, Circulation 141 (1) (2020) 42–66.
[26] I.A.M. Brown, L. Diederich, M.E. Good, L.J. DeLalio, S.A. Murphy, M.M. Cortese-Krott, et al., Vascular smooth muscle remodeling in conductive and resistance arteries in hypertension, Arterioscler. Thromb. Vasc. Biol. 38 (9) (2018) 1969–1985.
[27] M. Hristov, A. Zernecke, A. Schober, C. Weber, Adult progenitor cells in vascular remodeling during atherosclerosis, Biol. Chem. 389 (7) (2008) 837–844.
[28] M. Koenen, M.A. Hill, P. Cohen, J.R. Sowers, Obesity, adipose tissue and vascular dysfunction, Circ. Res. 128 (7) (2021) 951–968.
[29] L. Wang, J. Han, P. Shan, S. You, X. Chen, Y. Jin, et al., MD2 blockage protects obesity-induced vascular remodeling via activating AMPK/Nrf2, Obesity 25 (9) (2017) 1532–1539.
[30] J. Qian, W. Luo, C. Dai, J. Wang, X. Guan, C. Zou, et al., Myeloid differentiation protein 2 mediates angiotensin II-induced inflammation and mesenchymal transition in vascular endothelium, Biochim. Biophys. Acta, Mol. Basis Dis. 1867 (3) (2021), 166043.